Detection of hot electrons originating from an upper valley at ∼ 1.7 eV above the Γ valley in wurtzite GaN using electron emission spectroscopy

Wan Ying Ho, Abdullah I Alhassan, Cheyenne Lynsky, Yi Chao Chow, Daniel J Myers, Steven P Denbaars, Shuji Nakamura, Jacques Peretti, Claude Weisbuch, James S Speck

Detection of Hot Electrons Originating from an Upper Valley at ~1.7 eV above the Γ-valley in Wurtzite GaN using Electron Emission Spectroscopy (EES)

Wan Ying Ho,[1,a)] Abdullah I. Alhassan,[1] Cheyenne Lynsky,[1] Yi Chao Chow,[1] Daniel J. Myers,[1] Steven P. DenBaars,[1,2] Shuji Nakamura,[1,2] Jacques Peretti,[3] Claude Weisbuch,[1,3] and James S. Speck[1]

[1]*Materials Department, University of California, Santa Barbara, California 93106-5050, USA*

[2]*Department of Electrical and Computer Engineering, University of California, Santa Barbara, California 93106-5050, USA*

[3]*Laboratoire de Physique de la Matière Condensée, CNRS, Ecole Polytechnique, IP Paris, 91128 Palaiseau, France*

[a)]*wanying_ho@ucsb.edu*

Using Electron Emission Spectroscopy (EES), measurement and analysis were conducted on the energy distribution of vacuum emitted electrons from electrically driven InGaN/GaN green (peak wavelengths $\lambda \approx 515$ nm) light-emitting diodes (LEDs) with and without a pre-well superlattice (SL). We report on the detection of a high energy upper valley at ~1.7 eV above Γ-valley from samples with no pre-well SL. We propose that these upper valley electrons originate predominantly from trap-assisted Auger recombination (TAAR) in green LEDs, as the intensity of these peaks are found to have quadratic dependence on the carrier density, n (see Espenlaub *et al.*) [Espenlaub *et al.*, *Journal of Applied Physics* **126**, 184502 (2019)]. The high energy upper valley peak was not observed in the sample with a pre-well SL which is attributed to gettering by the pre-well SL of still unidentified impurities that act as TAAR centers.

While advances in light-emitting diodes (LEDs) have allowed their widespread use and application in the lighting industry, the technology still faces a major limitation posed by the "green gap" where the internal quantum efficiency (IQE) of LEDs decrease with increasing wavelength. The origins of the "green gap" are still under debate, with the increase in electron-hole separation decreasing radiative rates, while decreasing growth temperatures for the InGaN quantum wells may result in a high density of nonradiative recombination centers.[1–4]

At the same time, it is known that addition of an InGaN/GaN pre-well superlattice (SL) will improve the performance of green LEDs, though the reason for such improvement also remains an open question. These superlattices introduce V-defects that have been proposed improve hole injection through the V-defect sidewall.[5–7] The inclusion of SLs are also proposed to reduce Auger recombination;[8,9] or reduce defects and/or dislocations.[5,10] In most of these studies the authors correlate the pre-well SL with defect density and photo- or electroluminescence intensities, which ultimately are only indirect measurements of the nonradiative recombination processes.

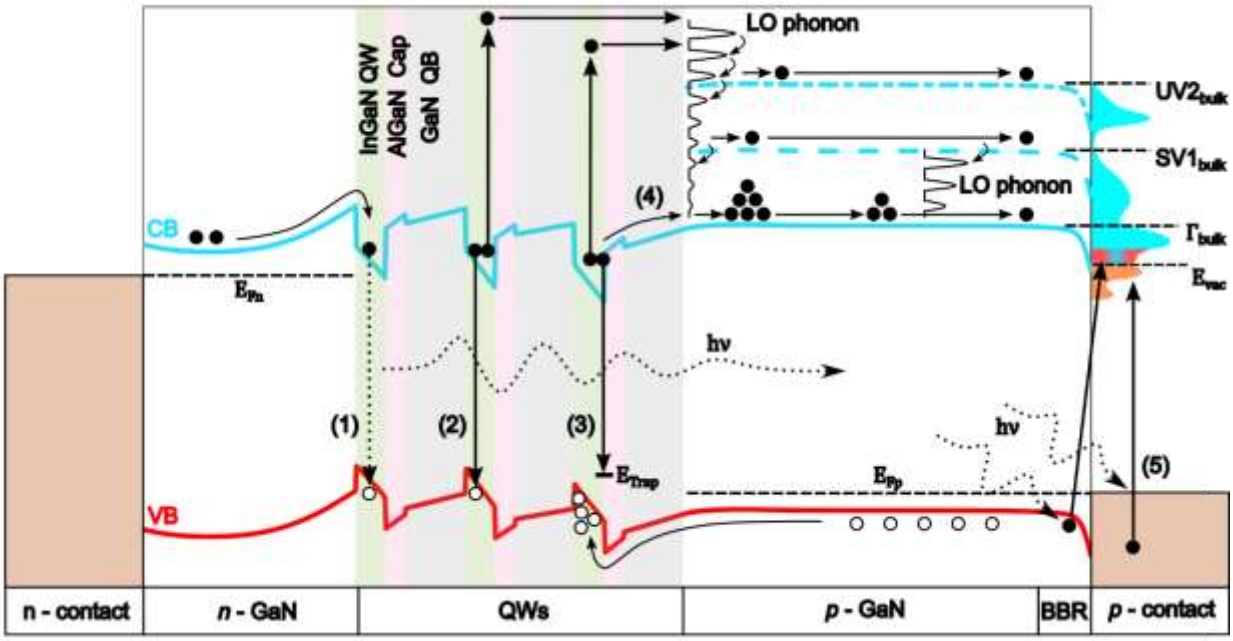

Figure 1: A schematic of the relevant electron energy levels, transport, recombination mechanisms, and the corresponding electron energy distribution curves in vacuum with (1) Radiative recombination, (2) band-to-band Auger recombination, (3) trap-assisted Auger recombination (TAAR), and (4) overflow. While three quantum wells are depicted, most of the recombination processes (1), (2) and (3) happen in the topmost quantum well (closest to the p-side of the junction) as it has the highest carrier density. The low energy peaks are generated by thermalized overflow or energy-relaxed hot electrons, photoemission of metal, and photoexcitation of electrons in the band-bending region (BBR)(5), both due to the LED light.

Electron Emission Spectroscopy (EES) of electrons emitted in vacuum enables direct measurement of hot electrons that are generated from Auger recombination processes in the active regions of heterostructures, including band-to-band Auger (electron-electron-hole, *eeh*) and trap-assisted Auger recombination (TAAR) (electron-electron, *ee*), as depicted in Fig. 1.[11–14] In such experiments, electrons originating from the active layers (darker region in Fig.1) are injected in the top *p*-layer of the structure. A fraction of these electrons survive transport towards the surface from which they exit into vacuum due to the cesiation of the *p*-layer into negative electron affinity (NEA). In this paper we observe hot electrons in EES spectra that accumulate in a new high energy GaN conduction band valley for LEDs without a pre-well SL and the suppression of these hot electrons with the inclusion of a pre-well SL.[11–14]

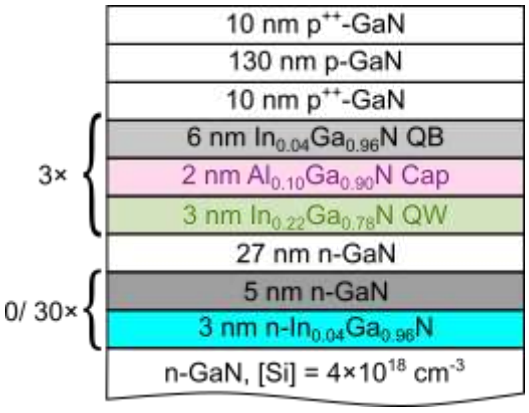

Figure 2: Schematic of the epi layer stack for the LEDs discussed in this work, grown by MOCVD (not to scale). The LEDs have different pre-well SL periods of 0 or 30 corresponding to total pre-well InGaN thicknesses of 0 and 90 nm respectively.

The green LEDs presented in this work were grown using metal-organic chemical vapor deposition (MOCVD) and were activated at 600 ºC. The samples were grown on top of a patterned sapphire substrate and an unintentionally-doped (UID) GaN buffer layer. The subsequent material consisted of an *n*-type GaN:Si layer ([Si] = 4×10^{18} cm^{-3}), 0 or 30 periods of *n*-type 5 nm $In_{0.04}Ga_{0.96}N$/3 nm GaN SL, a 3 period multiple quantum well (QW) with 3 nm $In_{0.22}Ga_{0.78}N$ QW/2 nm $Al_{0.10}Ga_{0.90}N$ cap layer/ 6 nm $In_{0.04}Ga_{0.96}N$ barriers), and 150 nm GaN:Mg ([Mg] = 5×10^{19} cm^{-3}) with a p^{++} contact layer ([Mg] = 2.5×10^{20} cm^{-3}). The epitaxial structures of the LEDs (henceforth referred as 0SL and 30SL corresponding to their SL period numbers) are shown in Fig. 2. The use of AlGaN cap layers had been shown to improve efficiency in longer wavelength LEDs by preventing desorption of the indium in QW during growth of the higher temperature barriers.[15]

The epitaxial materials were processed in parallel into devices suited for EES measurements.[16] The p-contact was 30 nm Pd/ 300 nm Au deposited in a honeycomb pattern, forming a single EES device of area 0.22 mm^2 with 0.096 mm^2 exposed p-GaN comprised of an array of hexagons with an apothem of 3.5 μm separated by 3 μm wide metal strips.[16] Each of the samples were cleaned and introduced into an ultra-high-vacuum (UHV) EES system as described in Ref. 11. For each sample a submonolayer of Cs was deposited (cesiation) using a SAES cesium source. By monitoring photoexcited electrons emitted from *p*-GaN during Cs deposition, we confirmed that NEA was achieved.[11] EES was performed with the devices biased under CW mode for injection currents ranging from 1 mA to 50 mA corresponding to current densities *J* ranging from 0.45 A

cm^{-2} to 22.5 A cm^{-2} - these current densities were chosen to be low to avoid self-heating without sacrificing signal-to-noise ratio. The energy of the emitted electrons was measured referenced to the Fermi level of the *p* contact using a Comstock AC-901 spherical sector electrostatic analyzer operated in constant pass energy mode with an energy resolution of 40 meV.[17] With increasing diode current, there was an increased ohmic voltage drop across the metal-semiconductor interface. This increased voltage drop shifted the measured energy of electrons emitted from the semiconductor surface to higher values but did not affect the Pd and Au photoemission peaks which are a result of diode light.[16,17] This voltage shift was employed to distinguish electrons originating from the semiconductor and to extract bulk valley minimum values at extrapolated zero bias.

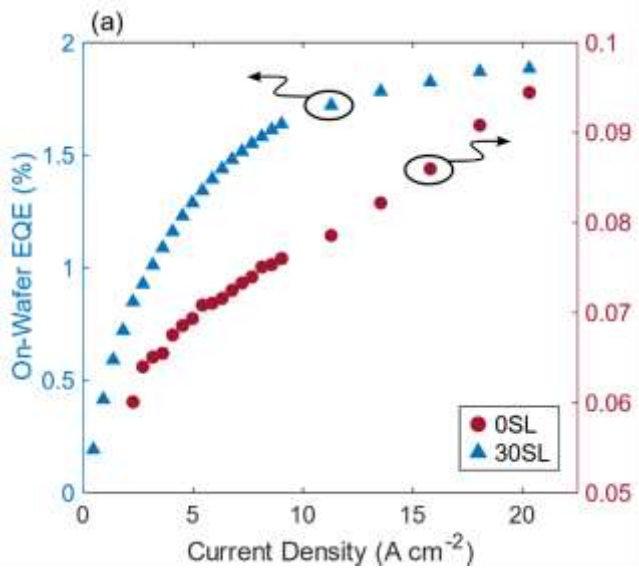
(a)
On-Wafer EQE (%)
Current Density (A cm^{-2})
0SL
30SL

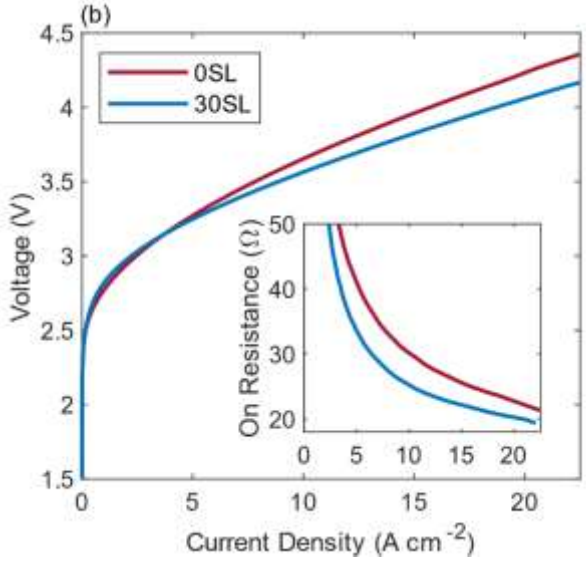
(b)
Voltage (V)
Current Density (A cm^{-2})
0SL
30SL
On Resistance (Ω)

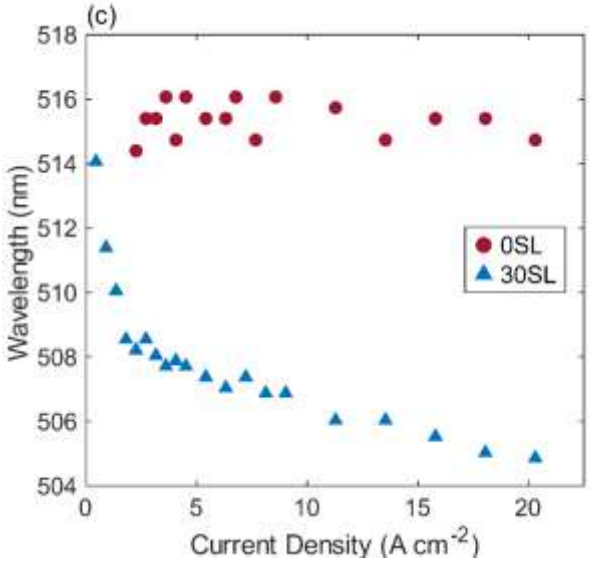
(c)
Wavelength (nm)
Current Density (A cm^{-2})
0SL
30SL

Figure 3: (a) Measured EQE of 0SL and 30SL devices as a function of current density. The EQE is shown to increase significantly with inclusion of pre-well SL. (b) Dependence of diode voltage and the on-resistances (inset) on current density. The inclusion of pre-well SL in the epitaxial structure reduced the operating voltages and on resistance. (c) Peak wavelength of 0SL and 30SL device as a function of current density.

The corresponding $J-V$, external quantum efficiency (EQE) and wavelength curves of the EES devices for the series were measured on die with a photodetector. The results are shown in Fig. 3 (a) – (c), with the on-resistances plotted as inset in Fig. 3 (b). The light output power (LOP) and hence the EQE markedly increased from 0SL to 30SL. The operating voltages improved as well. Circular transmission line measurements (CTLMs) demonstrated ohmic contact behavior to *p*-GaN for both samples, with similar specific contact resistivities in the low $10^{-3}\ \Omega\ \text{cm}^{-2}$ range. Hence the $J-V$ trends are not a result of contact resistances and originates from the semiconductor diode. This improvement in resistance may be attributed to reduced injection barriers at the sidewalls of V-defects, which are more numerous in the sample with pre-well SL.[18,19] Hence with addition of a pre-well SL the on resistance decreased. The current density at which the quantum efficiencies of these samples reached maximum, J^*, is lower for the sample with a pre-well SL, where $J^* \sim 22.5\ \text{A cm}^{-2}$ for 30SL and at $J^* > 450\ \text{A cm}^{-2}$ for 0SL. The current densities of the LEDs are given by:

$$J = J_{\text{SRH}} + J_{\text{rad}} + J_{\text{TAAR}} + J_{eeh\,\text{Auger}} + J_{\text{overflow}} \qquad (1)$$

$$= qd_{\text{QW}}(An + Bn^2 + B'n^2 + Cn^3) + J_{\text{overflow}}$$

where q is the elemental charge, d_{QW} is the thickness of the active region, and n is the carrier density of the active region. J_{SRH}, J_{rad}, J_{TAAR}, and $J_{eeh\,\text{Auger}}$ are Shockley-Read-Hall (SRH) recombination, radiative recombination, TAAR and *eeh* Auger recombination currents with

recombination coefficients A, B, B', and C, respectively. J_{overflow} correspond to overflow currents. The carrier density for peak EQE, $n^* = \sqrt{A/C}$ has corresponding current density, J^* given by:

$$J^* = qd_{\text{QW}}\left(2A\sqrt{\frac{A}{C}} + (B + B')\frac{A}{C}\right) + J_{\text{overflow}}. \quad (2)$$

Since the radiative and Auger recombination coefficients B and C are approximately the same for same active region designs, i.e., for these two samples, the high values for J^* are indicative of a large A coefficient and hence high SRH rates in these samples.[20–22] This can be attributed to the use of InGaN barriers, which are grown at lower temperatures than traditional GaN barriers. The overall reduction in J^* with inclusion of a pre-well SL indicates a reduction of SRH defects. The 30SL sample wavelength blue-shifted as expected when J increased due the free-carrier screening of internal electric field.[23] Reduced wavelength shift is observed for the 0SL sample. There, the high non-radiative recombination rate leads to lower carrier density, thus delaying the onset of free carrier screening of the polarization-related charges at the QW/quantum barrier interfaces.

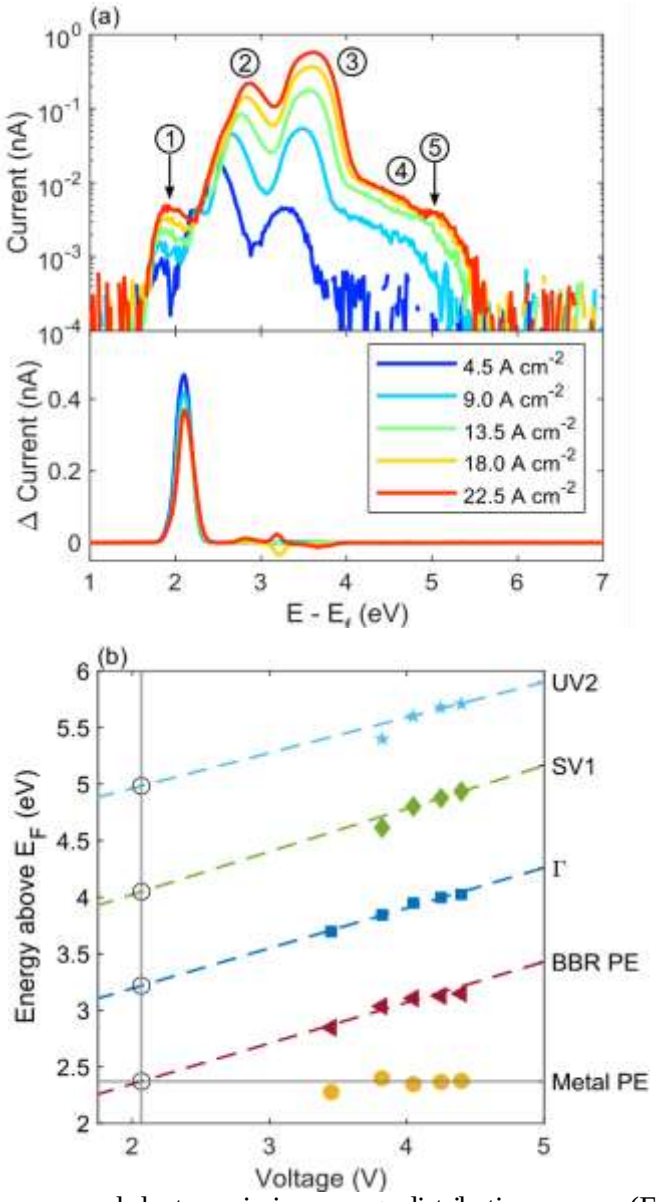

Figure 4: (a) Upper panel: measured electroemission energy distribution curves (EDCs, in terms of Faraday cup current) as shown in (a) for the 0SL sample at different current densities displaying 5 distinct peaks. Lower panel: differential photoemission EDCs measured when an external 532 nm laser was incident on the sample during LED operation (current injection), showing no significant change for peaks of semiconductor origin and only an increase in Au PE intensity. By extrapolating to the expected 0 mA position as shown in (b), the peaks are assigned to be arising from ① Au photoemission, ② photoexcitation from the BBR, ③ Γ-valley, ④ first side valley at ~0.9 *eV* above Γ, and ⑤ a higher energy peak of semiconductor origin at ~1.7 *eV* above Γ.

Let us focus on the energy distribution curves (EDCs) from EES under different currents of the 0SL sample shown in Fig. 4 (a) upper panel. The EDCs show five distinct peaks. The first peak ① remains constant in energy with increasing diode current and exhibits a linear correlation with LOP, which is characteristic of photoemission (PE) from Au of the p-contacts due to LED light.[16] A low energy peak ② below the conduction band minimum is identified as due to electrons originating from the band-bending region (BBR) (process(5) in Fig.1), photoemitted by Franz-Keldysh processes due to LED light.[14,24,25] Electrons excited to higher energies thermalize to the bottom of the conduction band valleys by emitting longitudinal-optical (LO) phonons. For peaks ③, ④, and ⑤ , the extracted high energy thresholds extrapolate to expected bulk valley minima at 0 mA of 3.22, 4.05 and 4.98 eV above Fermi level respectively as shown in Fig. 4 (b)[11,17] (see Supplementary Material for details). These values imply that peak ③ is comprised of electrons originating from the Γ-valley while peak ④ originates from the first side valley (SV).[11–14,16,17,24,26,27] The position of peak ⑤ increases with increasing the diode voltage and hence must originate from the semiconductor.[11,14] In the same line of reasoning with electrons in the first SV it is not possible to have electrons excited ~1.7 eV above the conduction band minimum by electric fields in the band bending region due to conservation of energy, thus these electrons originated form the active region.[28] Electrons that escaped the active region due to overflow from the active region will only end up in the Γ-valley and will mix with thermalized hot electrons.[28]

Let us discuss in more details the origin of peak ⑤: if it were due to a photoexcitation process, then by supplying additional photons on top of the LED light emission should increase the intensity of peak ⑤. We compared the measured 0SL EDCs with and without an external significantly brighter (than 0SL) 4.8 mW green laser of wavelength 532 nm (2.33 eV) incident on the sample.

A shown in Fig. 4 (a) lower panel that while metal photoemission increased by orders of magnitude, there is negligible change in the semiconductor peaks. Thus, we conclude that peak ⑤ originates from the semiconductor through electrical injection. As such, there are 5 total contributions observed – from metal photoemission, excitation from the BBR, Γ-valley, first side valley (SV1) at ~0.9 eV above Γ-valley, and an unidentified new peak of semiconductor origin at ~1.7 eV above Γ-valley which henceforth is referred to as upper valley (UV2). We note that the measured energy of UV2 is similar to a ~5.3 eV transition measured by optical reflectivity and ellipsometry,[29,30] but differs from theoretical calculations in regards to its energy relative to the Γ-valley.[29,31–35]

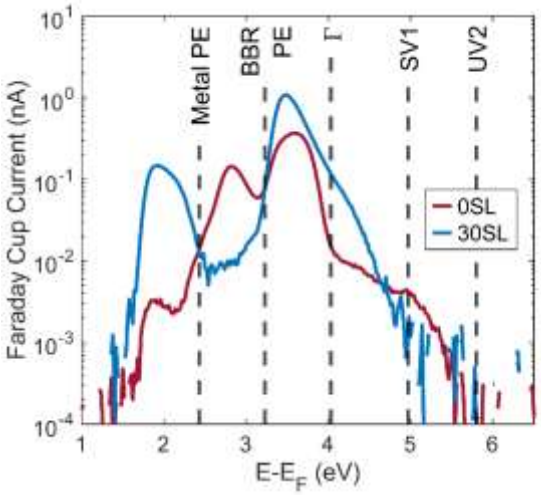

Figure 5: The EDCs measured at 22.5 A cm^{-2} are plotted with intensities scaled such that the Au PE peak intensity scales with LOP across samples. The peak identification lines (vertical dashed lines) are only a guide (see Fig. 3c and the supplementary material for the analysis of the peak position).

A comparison of the EDCs for both samples at 22.5 A cm^{-2} is plotted in Fig. 5. For the 30SL sample, three peaks were present with the peaks identified as Au PE, Γ-valley and SV1. As with the case for 0SL, a low energy peak below the Γ-valley peak is present for 30SL which is attributed

to the BBR.[14,24] Similar to previous reported EES measurements on various blue LEDs of different epitaxial structures, year of growth, and sources,[11–14,16,24,28] UV2 was not observed for 30SL.

The intensities of the various peaks were obtained by fitting superposed exponentially modified Gaussians to the EDCs using standard non-linear least squares method using OriginPro (see Supplementary Material for the fit of the 0SL EDC at 22.5 A cm^{-2}).[13] The equation for a single peak is given by:

$$f(x) = \frac{A}{\tau} e^{\frac{1}{2}\left(\frac{w}{\tau}\right)^2 - \frac{x - x_c}{\tau}} \int_{-\infty}^{z} \frac{1}{\sqrt{2\pi}} e^{-\frac{y^2}{2}} dy, \tag{3}$$

$$z = \frac{x - x_c}{w} - \frac{w}{\tau}$$

where A, x_c, w is the area, center, width of the peak, respectively, and τ is the exponent relaxation parameter.[12–14] From simulations detailed in the Supplementary Material, we found that the overflow current densities are low at less than 0.2% of the injected current for both samples at all investigated current densities, and hence will not contribute significantly to the Γ-valley peak intensities.[36–38] The possible origins of the electrons detected from the semiconductor valleys are hence *ee* TAAR or *eeh* Auger recombination.[11–14,21,24,28] In *ee* TAAR an electron is captured by a trap and the released energy excites another electron into higher valleys. Using the square root of Au PE peak intensity as a proxy for carrier density n in the active region a quantitative investigation of the peaks dependence on n can be performed.[13,14] Since the two samples have nominally identical active region structure, we can use the same radiative recombination coefficients B for both 0SL and 30SL such that $\sqrt{\text{Au PE Intensity}} \propto n$. If the valley is has predominant contributions from *ee* TAAR or *eeh* Auger generated electrons, its peak intensity will scale as n^2 or n^3, respectively.[12–14] If the valley has mixed contributions of both, we will expect

its peak intensity to have a power dependence between 2 and 3, or $ln(\text{Peak Intensity}) \propto \alpha\, ln(n)$ for a slope α where $2 \leq \alpha \leq 3$.

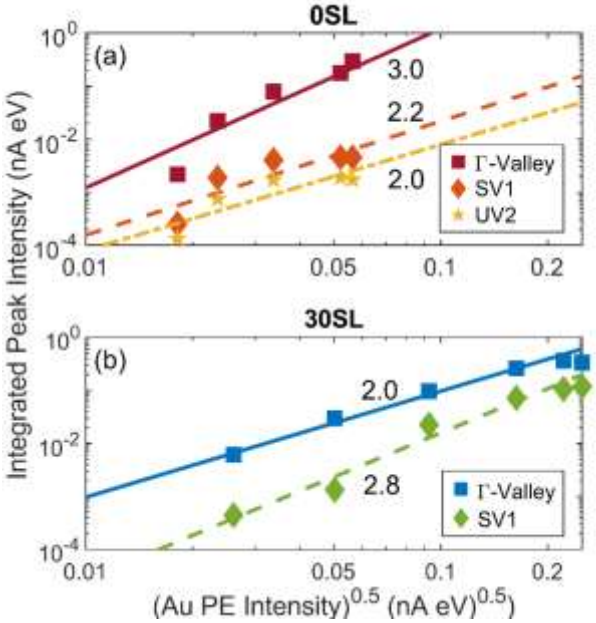

Figure 6: Using the square root of Au PE integrated intensity as a proxy for carrier density, n,[15,18] the peak intensities dependence of Γ-valley, SV1 and UV2 on $\sqrt{Bn^2}$ for 0SL and 30SL are plotted in (a) and (b), respectively. The slope of each line from bounded linear least square fits of the data are included. The slope of log-log plots gives the power dependence on n and hence indicate its origins. A slope of 2 corresponds to *ee* TAAR while a slope of 3 corresponds to *eeh* Auger recombination.

From the bounded least square fits as shown in Fig. 6, it was deduced that for 0SL Γ-valley, SV1 and UV2 have *eeh* Auger, mixed *eeh* Auger + *ee* TAAR, and *ee* TAAR contributions, respectively; while for 30SL, Γ-valley and SV1 have *ee* TAAR, and mixed contribution of *eeh* Auger + *ee* TAAR, respectively. The prominence of TAAR in these valleys is unsurprising as the EDCs are measured in the SRH dominant regime before peak EQE, where *ee* TAAR should be more dominant over *eeh* Auger. In the case of Γ-valley, the 3-body dependence implies that the

electrons may have scattered from the higher energy SV1 through intervalley scattering. However, it is also possible for these electrons to be excited directly by *eeh* Auger or *ee* TAAR and scattered into the Γ-valley.[14] For the SV1 and UV2 peaks, the traps involved in its generation by TAAR are most likely located at the AlGaN cap, which was shown to generate TAAR electrons even in a *p-i-n* device with an AlGaN EBL on the p-side of the junction.[13,14] These deep traps can be located at energies lower than 1.7 eV below the GaN conduction band minimum, thus providing enough energy for an electron to be excited at higher energies position and into UVs at different crystal momenta because of their very localized wavefunction, extended in k-space. It was observed that the peak intensity of the UV2 peak appears to saturate at higher current or carrier densities, which may be due to saturation of the defects involved in the TAAR events.

For the same J, LOP (or Au PE peak intensity) is much larger for 30SL. While the radiative and Auger recombination coefficients B and C are approximately the same for same active region designs, as discussed prior from the EQE peak position J^*, A is much smaller for 30SL. Since TAAR pathways scale as trap density, as indicated by the absence of UV2 in 30SL's EDCs, B' is also smaller for 30SL. Hence at the same current densities, n must be larger for 30SL. This leads to larger TAAR current and *eeh* Auger recombination currents, corresponding to larger Γ-valley and SV1 peak intensities, respectively, in the 30SL sample.

The observation that with addition of a pre-well SL (i) A decreases and (ii) total TAAR rate decreases is consistent with the claim that pre-well InGaN layers reduce the concentration of nonradiative recombination centers in the active region.[10] It should be noticed that, in blue LEDs, the UV2 peak at ~ 1.7 eV above Γ is not observed in devices with thin pre-well SL as in Ref. 14 or even in devices without pre-well SL. However, there are three major differences between the measured sample in Ref. 14 and the green LEDs reported here. First, the LEDs in Ref. 14 have

many more quantum wells, part of which may partially perform the same function as the pre-well SLs; and secondly, the indium content is smaller in the blue wells. It has been proposed that the green gap was caused, in part, by TAAR which is exacerbated by the higher point defect density in green wells (higher In composition).[4] It is possible that the blue LEDs have smaller point defect densities which can act as TAAR pathways. The reason why UV2 is not observed in usual blue LEDs although its energy level lies within reach of *eeh* Auger electrons is not identified at the moment. We speculate that it relies on an interband Auger transition, usually forbidden for conduction electrons near Γ zone center, but which might become allowed for highly localized TAAR centers.[39] As such, the initial energy and momentum of the TAAR excited electron, as well as its subsequent pathway into an upper valley may be different from that of hot electrons generated by 3-body Auger recombination. More systematic studies of defect-related peaks would be needed to put this on firmer ground.

In conclusion, we have measured hot electrons emitted from green LEDs with and without pre-well SL and quantitatively analyzed their origins. We have shown that in these green LEDs Γ-valley and SV1 electrons are generated by TAAR and *eeh* Auger processes, while there is significant overflow electrons contributing to Γ-valley for the sample with a pre-well SL due to higher active region carrier densities.[14] We have detected hot electrons from a higher energy side valley, in addition to those from the conduction band minimum and first side valley, which is located at ~1.7 eV above the conduction band minimum. Electrons excited to the higher energy side valley are due to TAAR processes. These results agree with the proposition that a pre-well InGaN suppresses defects in the active region, hence with a pre-well SL the TAAR generated UV2 peak decreased in intensity.[10]

Support at UCSB was provided by the Solid State Lighting and Energy Electronics Center (SSLEEC); the University of California, Santa Barbara (UCSB) – Collaborative Research of Engineering, Science and Technology (CREST) program; U.S. Department of Energy under the Office of Energy Efficiency & Renewable Energy (EERE) Award Nos. DE-EE0007096 and DE-EE0009691; the Simons Foundation (Grant #s 601952 and 601954 for JSS and CW, respectively); the National Science Foundation (NSF) RAISE program (Grant No. DMS-1839077 for JSS and CW); and Sandia National Laboratory (Award # 2150283). A portion of this work was performed at the UCSB Nanofabrication facility.

References

[1] A.M. Armstrong, B.N. Bryant, M.H. Crawford, D.D. Koleske, S.R. Lee, and J.J. Wierer, J. Appl. Phys. **117**, 134501 (2015).
[2] S. Schulz, M.A. Caro, C. Coughlan, and E.P. O'Reilly, Phys. Rev. B **91**, 035439 (2015).
[3] M. Auf der Maur, A. Pecchia, G. Penazzi, W. Rodrigues, and A. Di Carlo, Phys. Rev. Lett. **116**, 027401 (2016).
[4] A. David, N.G. Young, C.A. Hurni, and M.D. Craven, Phys. Rev. Applied **11**, 031001(R) (2019).
[5] V.S. Sizov, A.F. Tsatsulnikov, A.V. Sakharov, W.V. Lundin, E.E. Zavarin, N.A. Cherkashin, M.J. Hÿtch, A.E. Nikolaev, A.M. Mintairov, Y. He, and J.L. Merz, Semiconductors **44**, 924 (2010).
[6] X. Wu, J. Liu, Z. Quan, C. Xiong, C. Zheng, J. Zhang, Q. Mao, and F. Jiang, Appl. Phys. Lett. **104**, 221101 (2014).
[7] M. Liu, J. Zhao, S. Zhou, Y. Gao, J. Hu, X. Liu, and X. Ding, Nanomaterials **8**, 450 (2018).
[8] I.A. Prudaev, I.S. Romanov, V.V. Kopyev, V.N. Brudnyi, A.A. Marmalyuk, V.A. Kureshov, D.R. Sabitov, and A.V. Mazalov, Russ Phys J **59**, 934 (2016).
[9] C. Jia, T. Yu, H. Lu, C. Zhong, Y. Sun, Y. Tong, and G. Zhang, Opt. Express **21**, 8444 (2013).
[10] C. Haller, J.-F. Carlin, G. Jacopin, D. Martin, R. Butté, and N. Grandjean, Appl. Phys. Lett. **111**, 262101 (2017).
[11] J. Iveland, L. Martinelli, J. Peretti, J.S. Speck, and C. Weisbuch, Phys. Rev. Lett. **110**, 177406 (2013).
[12] D.J. Myers, A.C. Espenlaub, K. Gelzinyte, E.C. Young, L. Martinelli, J. Peretti, C. Weisbuch, and J.S. Speck, Appl. Phys. Lett. **116**, 091102 (2020).
[13] D.J. Myers, K. Gelžinytė, A.I. Alhassan, L. Martinelli, J. Peretti, S. Nakamura, C. Weisbuch, and J.S. Speck, Phys. Rev. B **100**, 125303 (2019).
[14] W.Y. Ho, Y.C. Chow, D.J. Myers, F. Wu, J. Peretti, C. Weisbuch, and J.S. Speck, Appl. Phys. Lett. **119**, 051105 (2021).
[15] A.I. Alhassan, R.M. Farrell, B. Saifaddin, A. Mughal, F. Wu, S.P. DenBaars, S. Nakamura, and J.S. Speck, Opt. Express **24**, 17868 (2016).
[16] D.J. Myers, K. Gelžinytė, W.Y. Ho, J. Iveland, L. Martinelli, J. Peretti, C. Weisbuch, and J.S. Speck, Journal of Applied Physics **124**, 055703 (2018).
[17] J. Iveland, M. Piccardo, L. Martinelli, J. Peretti, J.W. Choi, N. Young, S. Nakamura, J.S. Speck, and C. Weisbuch, Appl. Phys. Lett. **105**, 052103 (2014).
[18] N. Okada, H. Kashihara, K. Sugimoto, Y. Yamada, and K. Tadatomo, Journal of Applied Physics **117**, 025708 (2015).
[19] Q. Lv, J. Liu, C. Mo, J. Zhang, X. Wu, Q. Wu, and F. Jiang, ACS Photonics **6**, 130 (2019).
[20] Q. Dai, Q. Shan, J. Wang, S. Chhajed, J. Cho, E.F. Schubert, M.H. Crawford, D.D. Koleske, M.-H. Kim, and Y. Park, Appl. Phys. Lett. **97**, 133507 (2010).
[21] A.C. Espenlaub, D.J. Myers, E.C. Young, S. Marcinkevičius, C. Weisbuch, and J.S. Speck, Journal of Applied Physics **126**, 184502 (2019).
[22] K.A. Bulashevich, O.V. Khokhlev, I.Yu. Evstratov, and S.Y. Karpov, in edited by K.P. Streubel, H. Jeon, L.-W. Tu, and N. Linder (San Francisco, California, USA, 2012), p. 827819.
[23] S. Chichibu, T. Azuhata, T. Sota, and S. Nakamura, Appl. Phys. Lett. **69**, 4188 (1996).
[24] M. Piccardo, L. Martinelli, J. Iveland, N. Young, S.P. DenBaars, S. Nakamura, J.S. Speck, C. Weisbuch, and J. Peretti, Phys. Rev. B **89**, 235124 (2014).
[25] M. Sauty, N.M.S. Lopes, J.-P. Banon, Y. Lassailly, L. Martinelli, A. Alhassan, S. Nakamura, J.S. Speck, C. Weisbuch, and J. Peretti, (2022).
[26] S. Marcinkevičius, T.K. Uždavinys, H.M. Foronda, D.A. Cohen, C. Weisbuch, and J.S. Speck, Phys. Rev. B **94**, 235205 (2016).
[27] S. Wu, P. Geiser, J. Jun, J. Karpinski, D. Wang, and R. Sobolewski, Journal of Applied Physics **101**, 043701 (2007).
[28] J. Peretti, C. Weisbuch, J. Iveland, M. Piccardo, L. Martinelli, and J.S. Speck, in edited by K.P. Streubel, H. Jeon, L.-W. Tu, and M. Strassburg (San Francisco, California, United States, 2014), p. 90030Z.
[29] S. Bloom, G. Harbeke, E. Meier, and I.B. Ortenburger, phys. stat. sol. (b) **66**, 161 (1974).
[30] R. Goldhahn, K. Lange, and M. Feneberg, in edited by J.-I. Chyi, H. Fujioka, and H. Morkoç (San Francisco, California, United States, 2015), p. 93630G.
[31] D. Fritsch, H. Schmidt, and M. Grundmann, Phys. Rev. B **67**, 235205 (2003).
[32] B. Rezaei, A. Asgari, and M. Kalafi, Physica B: Condensed Matter **371**, 107 (2006).
[33] L.C. de Carvalho, A. Schleife, and F. Bechstedt, Phys. Rev. B **84**, 195105 (2011).
[34] M.A. Caro, S. Schulz, and E.P. O'Reilly, Phys. Rev. B **88**, 214103 (2013).
[35] Q. Yan, P. Rinke, A. Janotti, M. Scheffler, and C.G. Van de Walle, Phys. Rev. B **90**, 125118 (2014).

[36] C.-K. Li, M. Piccardo, L.-S. Lu, S. Mayboroda, L. Martinelli, J. Peretti, J.S. Speck, C. Weisbuch, M. Filoche, and Y.-R. Wu, Phys. Rev. B **95**, 144206 (2017).
[37] H.K. Gummel, IEEE Trans. Electron Devices **11**, 455 (1964).
[38] D.N. Arnold, G. David, D. Jerison, S. Mayboroda, and M. Filoche, Phys. Rev. Lett. **116**, 056602 (2016).
[39] E. Kioupakis, P. Rinke, A. Schleife, F. Bechstedt, and C.G. Van de Walle, Phys. Rev. B **81**, 241201(R) (2010).